Journal of Biomedical Optics 9(6), 1320–1326 (November/December 2004)

Comparison between ultraviolet-visible and near-infrared elastic scattering spectroscopy of chemically induced melanomas in an animal model

Ousama M. A'Amar
Boston University
Department of Biomedical Engineering
Boston, Massachusetts 02215

Ronald D. Ley
University of New Mexico
School of Medicine
Albuquerque, New Mexico 87131

Irving J. Bigio
Boston University
Department of Biomedical Engineering
Boston, Massachusetts 02215

Abstract. The work reported compares elastic scattering spectroscopy (ESS) for diagnosis of pigmented skin lesions in two spectral regions: UV-visible and near infrared (NIR). Given the known strong absorption by melanin in the near-UV to mid-visible range of the spectrum, such a comparison can help determine the optimum wavelength range of ESS for diagnosis of pigmented skin lesions. For this purpose, four South American opossums are treated with dimethylbenz(a)anthracene on multiple dorsal sites to induce both malignant melanomas and benign pigmented lesions. Skin lesions are examined *in vivo* with ESS using both UV-visible and NIR, with wavelength ranges of 330 to 900 nm and 900 to 1700 nm, respectively. Both portable systems use the same fiber optic probe geometry. ESS measurements are made on the lesions, and spectral differences are grouped by diagnosis from standard histopathological procedure. Both ESS datasets show strong spectral trends with the histopathological assignments, and the data suggest a model for the underlying basis of the spectral distinction between benign and malignant pigmented nevi. [DOI: 10.1117/1.1803845]

Keywords: cancer diagnosis; fiber optic probe; elastic scattering spectroscopy; melanoma; optical biopsy.

Paper 03096 received Jul. 15, 2003; revised manuscript received Jan. 23, 2004; accepted for publication Apr. 2, 2004. This paper is a revision of a paper presented at the SPIE conference on Biomedical Diagnostic, Guidance, and Surgical-Assist Systems III, Jan. 2001, San Jose, California. The paper presented there appears (unrefereed) in SPIE Proceedings Vol. 4254.

1 Introduction

The mortality rate due to cutaneous malignant melanoma has grown over the past 20 years in most parts of the world.[1–3] Successful treatment of melanoma depends on early diagnosis and excision. Prior to excision, the diagnostic accuracy of identifying a pigmented skin lesion as malignant or benign depends essentially on the practitioner expertise. Some pigmented skin lesions are difficult to classify, especially when they present unusual features.[4] Chen et al. have reported that the probability of primary-care physicians to correctly determine that a pigmented lesion may be malignant and to make the appropriate management decision (either to order a biopsy or to refer the patient to a melanoma specialist) can be as low as 0.42.[5] Melanoma can be sometimes confused, even for the skin-cancer specialist, with other types of pigmented lesions (melanocytic nevi).[6] Early melanoma diagnosis is mostly based on the visual features of the suspected lesions such as the asymmetry, border, color, and dimension (ABCD).[7] Several computerized imaging techniques that could help in recognizing these criteria have been developed. Applying the ABCD criteria, a spectrophotometric imaging technique that uses selected spectral bands from 420 to 1040 nm to enhance the ABCD criteria (and mainly the color of the suspected lesions) has been shown to improve the accuracy of detecting melanoma.[8–10] Dermoscopy, an imaging technique that is used extensively in clinical practice, can enhance the detection of microscopic features (e.g., brown globules, pigment network, branched streak, and homogeneous blue pigmentation) of cutaneous melanocytic lesions.[11,12] Dermoscopy has shown higher sensitivity values (90 to 95%) compared with the average sensitivity (70 to 80%) for clinical visual examination.[13] However, the specificity (correctly identifying benign lesions) is still poor. A fiber optic confocal imaging system, with associated fluorescent markers, has been tested on an animal model and was sensitive to melanoma tumors up to 0.2 mm under the skin surface.[14]

Recent advances in several areas of optical technology have led to the development of a variety of optical biopsy techniques. These techniques offer a range of modalities for diagnosis, and include elastic scattering spectroscopy (ESS), light-induced fluorescence spectroscopy (LIFS)[15–17] optical coherence tomography (OCT),[18–20] diffuse optical tomography (DOT),[21–23] and Raman and vibrational spectroscopy.[24–26] ESS, sometimes called diffuse-reflectance spectroscopy,[27] is a particularly attractive technique, since it provides spectra that contain information about the subcellular morphology of the tissue as well as the chromophore con-

Address all correspondence to Ousama M. A'Amar, Boston Univ., Department of Biomedical Engineering, c/o Department of Electrical and Computer Engineering, Photonics Bldg., 8 St. Mary's Street, Boston, MA 02215. Tel: 1-617-353-0261; Fax: 1-617-353-1283; E-mail: oaamar@bu.edu

1083-3668/2004/$15.00 © 2004 SPIE

tent (e.g., hemoglobin and melanin).[28] Because ESS translates tissue morphological changes at the cellular and subcellular level into spectral features,[29] it can be compared with standard histopathologic assessment, which is commonly based on the analysis of microscopic structure.[16,30] Hence, ESS may be an appropriate technique for cancer diagnosis, with the advantage of noninvasively providing real-time diagnostic signatures *in situ*, which are related to histopathology.

We have previously reported on clinical studies using the ESS technique for diagnosing breast tissues and breast sentinel lymph nodes,[31] upper and lower GI tract mucosa,[32,33] and bladder.[34] This work focuses on the problem of pigmented skin lesions for which standard histopathologic examination is the best method available for determining the presence or absence of melanoma.[35]

The progression of the melanocyte to a malignant melanoma passes through various steps: development of benign nevocellular nevus, preneoplastic dysplastic nevus, primary melanoma, and metastatic melanoma.[36] The thickness, known as the Breslow thickness, of the lesion is an important prognostic factor for melanocytic lesions.[37–39] Differences in lesion thickness and microscopic architecture changes are both likely to affect the ESS signal. Over the red to near-infrared spectral region, scattering dominates over absorption in most tissue,[16,40,41] with hemoglobin having a stronger absorption effect at wavelengths under 600 nm, especially for subepithelial tissues. However, pigmented skin lesions, both malignant and benign, generally contain higher concentrations of melanin than normal skin. Melanin is known to absorb and scatter light very strongly in the UV-visible spectral region, with the extinction coefficient rising for shorter wavelengths as result of Rayleigh scattering caused by the melanin granules.[42] The absorption of melanin is much weaker in the near-infrared (NIR), where scattering can be expected to dominate in skin.

Optical properties of melanoma have been explored using reflectance spectroscopy. Using a bundle of 30 fiber optics (18 sources and 12 detector) as a probe, Wallace et al. recorded the reflectance spectra (320 to 1100 nm) from 121 melanocytic benign and malignant skin lesions.[43] Encouraging correlations with pathology were reported. The accuracy of detecting melanomas was either 72 or 86.7% based on the classification method used for the analysis of the spectra.[44] McIntosh et al. have performed *in vivo* reflectance spectroscopy (400 to 2500 nm) on skin neoplasms (both pigmented and nonpigmented lesions). Significant spectral differences ($p<0.05$) were found between normal skin and skin neoplasms in several regions of the NIR spectrum.[45]

To our knowledge no one has reported on the use of ESS on melanoma beyond the wavelength 1100 nm. Given the strong absorption by melanin at the shorter wavelengths, it is instructive to compare spectra obtained by the ESS method using our previously employed instrumentation over the spectral range 330 to 900 nm, with spectra extending farther into the NIR (900 to 1700 nm). The intent is to be more sensitive to changes in scattering that accompany dysplasia, rather than being mainly sensitive to the presence of major absorbers (e.g., hemoglobin and melanin). Therefore, we deemed it warranted to explore pigmented lesions using the NIR spectral region to determine which spectral range would be more effective for distinguishing malignant from benign conditions in pigmented skin lesions. For this purpose, four opossums were treated with dimethylbenz(a)anthracene to induce malignant melanomas as well as benign pigmented lesions. 13 pigmented lesions were examined *in vivo* using both UV-visible and NIR-ESS, and subjected to histopathological assessment. It is recognized that such a small number cannot constitute the basis of statistical analysis, so the goal of this study was to assess quantitatively the strength of correlation with histopathology for two wavelength ranges of ESS, and to provide guidance for larger studies.

2 Materials and Methods

2.1 *Animals*

Animals were from the breeding colony maintained at the Southwest Foundation for Biomedical Research (San Antonio, Texas). The University of New Mexico Institutional Animal Care and Use Committee approved protocols were used in this study. Opossum skin (for this breed) is thin compared to human skin. Normal opossum skin of the torso (both ventral and dorsal surfaces) lacks Rete ridges. The stratum basale and stratum spinosum together are 1 to 4 cells thick; the stratum granulosum is discontinuous, and the stratum corneum is relatively thick and of uniform thickness.[46] Therefore, this animal model is suitable for scattering measurements.

2.2 *Treatment with 7, 12-Dimethylbenz(a)anthracene*

Prior to treatment, animals were anesthetized in a halothane/O_2 atmosphere and dorsal hair was removed. The shaved dorsum of eight opossums was treated with 100 μl of 0.5% dimethylbenz(a)anthracene (DMBA) in ethanol on Monday and Thursday of week 1. At week 9, the average number of melanocytic lesions greater than 1 mm in diameter per animal was approximately 12. One or more of these lesions on each animal progressed over a 2-yr period to melanomas. Melanomas on three of the animals had metastasized to lymph nodes, liver, spleen, and lungs. 76 weeks following DMBA treatment, a total of 13 melanocytic lesions on four of the surviving five animals were analyzed by ESS while animals were anesthetized. The lesions appeared to the unaided eye to be uniformly pigmented and quite dark. The lateral size of the lesions ranged between 3 and 7 mm in diameter. Comparable colors and sizes were observed for both benign and melanoma lesions.

2.3 *Histopathology*

Following ESS measurements, and while the animals were anesthetized, 13 melanocytic lesions were removed for histopathologic examination. The samples were fixed in 10% neutral buffered formalin, embedded in paraffin, sectioned at 5 μm, and stained with hematoxylin and eosin. Following microscopic examination, the lesions were classified as melanomas or benign lesions based on cellular morphology.

2.4 *ESS Systems*

The general principles of elastic scattering spectroscopy and the operating features of the optical systems have been described in earlier publications.[32,34] Although not previously described in those publications, the NIR system invokes a different spectrometer (Control Development, Incorporated, South Bend, Indiana) and light source, but operates in the

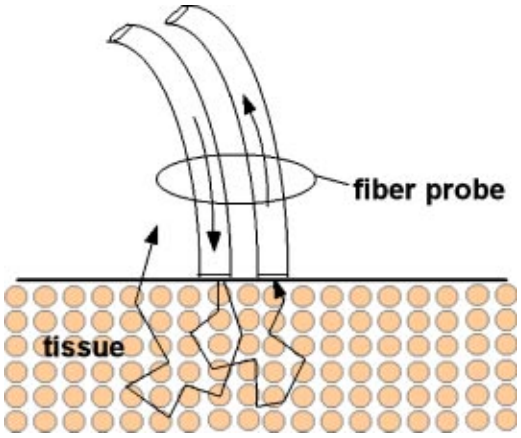

Fig. 1 A schematic diagram showing the optical geometry of the fiber probe used in optical contact with the tissue for elastic scattering spectroscopy.

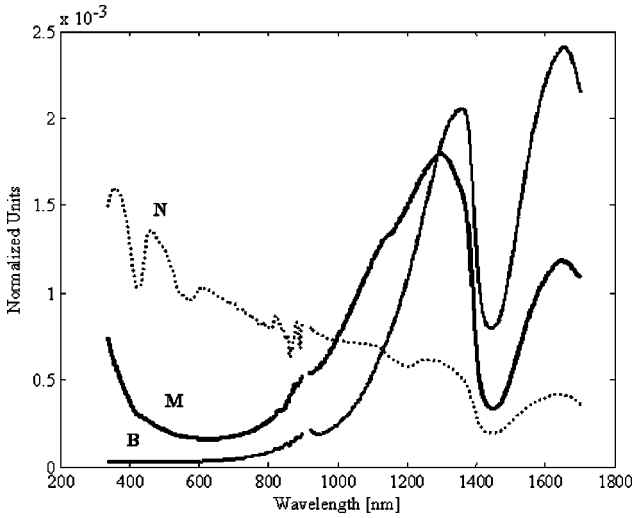

Fig. 2 Normalized elastic scattering spectra representative of typical data for pigmented benign lesions, melanomas, and normal skin measured on opossums using UV-visible ESS system. B is benign pigmented lesion. M is melanoma, N is normal skin.

same manner as the UV-visible system. It is integrated into a portable computer chassis, and has no moving parts. The spectrometer utilizes a single-stage TE cooled 512-element InGaAs array for detection and appropriately specified mirrors, grating, etc. The UV-visible system uses a pulsed broadband Xenon arc lamp as the light source, and the system response covers the spectral range of 330 to 900 nm. The NIR light source is a continuous broadband incandescent lamp, which easily covers the detector's spectral region of 900 to 1700 nm. Both systems use the same fiber optic probe geometry. The core diameters for illuminating and collecting fibers were 400 and 200 μm, respectively, with center-to-center separation of 350 μm, and spectra are taken with the probe tip in optical contact with the tissue surface (see Fig. 1). At this small separation, the collected light is highly sensitive to scattering but is also sensitive to absorption properties of tissue.[47,48] With this configuration, collected scattered light must undergo one to several scattering events at a typical depth (in the UV-visible region) of between 100 and 400 μm from the surface of the lesion. For the specific probe geometry used in this work, our Monte Carlo simulations showed that collected photons from tissue in the NIR region, beyond the absorption peaks of water, come from a depth of up to 750 μm, although many photons are collected from shallow depths. Assuming the typical banana-shaped zone of the scattered photons between the illumination (400 μm) and the collection (200 μm) fibers, the volume investigated ranges approximately between 0.06 mm^3 (UV-visible) and 0.2 mm^3 (NIR).

At least three measurements were taken on a specific area of each lesion, and then averaged to represent the ESS spectrum for that lesion. The sites on the lesions where the measurements were taken were precisely marked for the histopathological assessment. All measurements reported in this work were taken in the presence of ambient illumination with background subtraction, and the spectral response of each system was calibrated by recording a reference spectrum from a spectrally flat diffuse reflector (Spectralon®). Thus, the displayed spectra were calculated according to:

$$I(\lambda)=\frac{I(\lambda)_{\text{tissue}}-I(\lambda)_{\text{tissue background}}}{I(\lambda)_{\text{ref}}-I(\lambda)_{\text{ref backround}}}.$$

2.5 *Mathematical Treatment of Data*

The resulting spectra $I(\lambda)$ were normalized to the total area under the entire curve to facilitate comparison of spectral shapes. In the UV-visible ESS, the area difference between the trapezoid formed at the boundaries of the range of 400 to 650 nm and the corresponding spectral curve was used as the criterion to distinguish malignant melanomas from benign lesions. The NIR-ESS spectra were renormalized to unity at the wavelength 1340 nm, chosen because there is minimal water absorption at this wavelength. The area under the curve covering the range of 920 to 1200 nm in the normalized spectra served as the distinction criterion.

3 Results and Discussion

The 13 biopsied lesions were analyzed by standard histopathological criteria, assessing the cellular morphology. Using these criteria, the samples were classified as follows: 5 melanomas, 1 undecided (indeterminate), 6 benign lesions, and 1 normal skin.

Typical spectra from both the UV-visible and NIR ESS systems, for pigmented benign lesions, melanomas, and normal skin, are shown in Fig. 2. The normalized spectral intensities were adjusted so that the intensities at 900 nm in the UV-visible spectra meet the starting intensities at 920 nm in NIR spectra. These resulting spectra were then normalized again to have the same total area under the curve, and each represents the average of the three types of all spectra for the corresponding diagnosis.

As shown in Fig. 2, the chromophores that affect the ESS spectra, in both UV-visible and NIR spectral regions, are melanin, hemoglobin, and water. Melanin, which strongly absorbs light in the UV-visible region, is the major chromophore in the pigmented lesions.[41,42] The extinction spectrum of

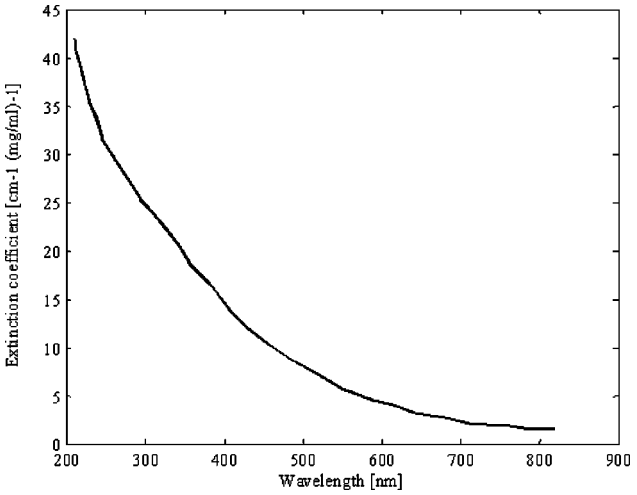

Fig. 3 Extinction spectrum of eumelanin. The data for this spectrum were obtained from the Laper Photomedicine and Biomedical Optics at the Oregon Medical Center web pages (http://omlc.ogi.edu). They refer to Ref. 49 as their source of data.

eumelanin[49] (the class of melanin found in human black hair) is shown in Fig. 3. If the absorption process due to melanin was always dominant, the spectral region from 330 to 600 nm would be expected to be strongly attenuated. Figure 4(a) shows a close view of the ESS spectra in the UV-visible range. The error bars represent typical range of deviation (min to max) from the mean value of ESS traces in the regions of interest (400 to 650 nm and 920 to 1200 nm) for malignant (bold line) and benign (thin line) lesions. The full range of deviation in the spectral regions of interest is reflected in Fig. 5.

The shape of the ESS spectra for melanoma for the short-wavelength range of the spectrum, 330 to 600 nm, is surprising. Although melanin absorbs very strongly in this region, with the extinction coefficient rising for shorter wavelengths, the ESS signal actually increases. In contrast, the ESS signal from benign pigmented lesions either decreases, as expected, for shorter wavelengths, or exhibits only a slight rise. For melanomas, the scattering appears to increase sufficiently at shorter wavelengths to overtake the effect of increasing absorption.

A strong source of scattering in melanocytic lesions is the melanosomes. In the opossum melanomas, the melanosomes are generally oval ($\sim 0.5 \times 0.3\ \mu$m), solitary, and not clustered in compound melanosomes.[50] Their size range overlaps that found for melanosomes in humans.[51,52] The scatterers' size is comparable to the wavelengths in the UV-visible region (330 to 900) and a few times smaller than the wavelengths in the NIR (900 to 1700 nm). Given that the probe geometry used in ESS is sensitive to both scattering and absorption, this suggests that the change in scattering properties of the melanosomes and/or melanin (and/or other subcellular changes) has a stronger effect on the shape of the spectrum (for the shorter wavelengths) than the chromophore content in pigmented melanomas. This is consistent with the interpretation that melanosomes and melanin granules in malignant lesions act more strongly as Mie and Rayleigh scatterers than is the case in benign pigmented lesions. It also agrees with the

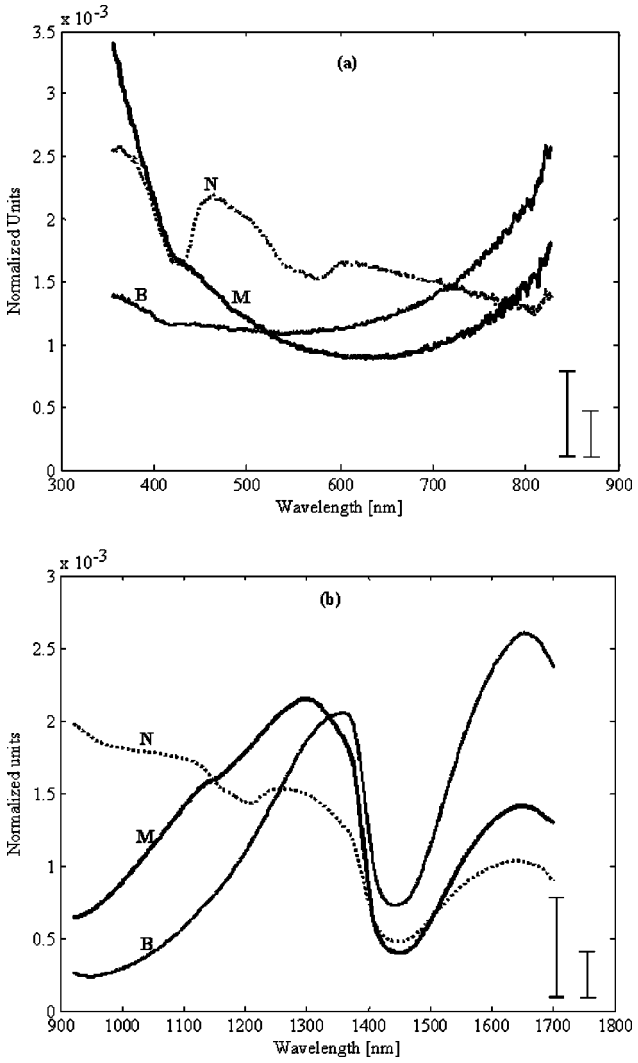

Fig. 4 Close view of the normalized elastic scattering spectra representative of typical data for pigmented benign lesions, melanomas, and normal skin measured on opossums using (a) UV-visible and (b) NIR ESS systems. B is benign pigmented lesion, M is melanoma, and N is normal skin. The error bars represent typical range of deviation (min to max) from the mean value of ESS traces in the regions of interest (400 to 650 nm and 920 to 1200 nm) for malignant (bold line) and benign (thin line) lesions.

findings of Wolbarsht, Walsh, and George, in which they showed that, in addition to absorption properties, the melanin granules act as strong Rayleigh scattering centers[42] (due to their large refractive index). This hypothesis is further supported by the fact that we were able to observe a slight absorption feature of the hemoglobin Soret-band ($\approx$416 nm) in the melanoma lesions, which was not overwhelmed by the weaker-than-expected absorption by melanin.

The normal skin spectrum shows obvious features due to hemoglobin absorption bands ($\approx$416, 540, and 580 nm). It is noted that the normal skin of this animal model contains little melanin, which is evident from the spectra. In humans, however, there can be significant levels of melanin in normal skin, and in such cases typical ESS spectra, with the same geometry, always exhibit strong absorption due to melanin at the shorter wavelengths, with less evidence of enhanced scatter-

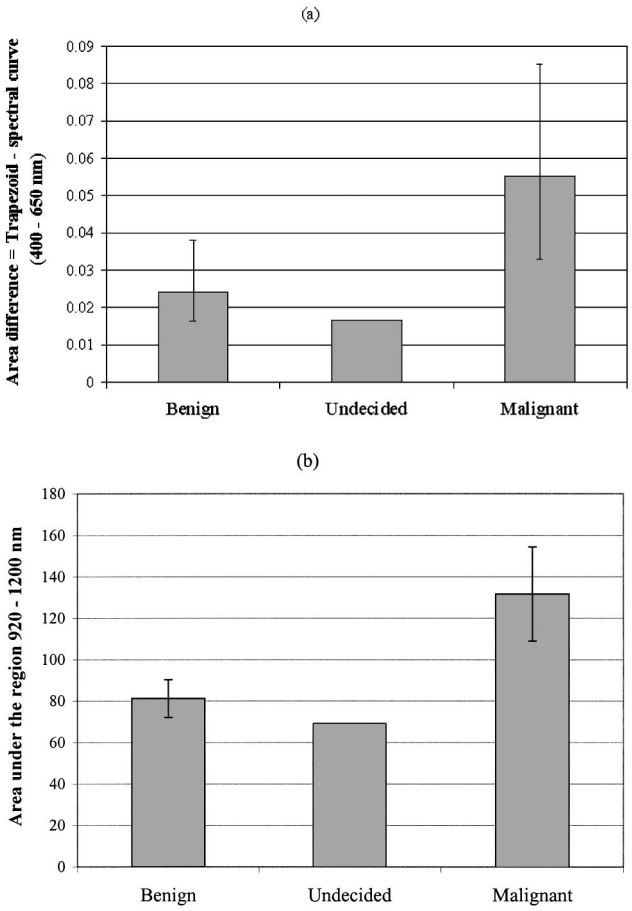

Fig. 5 Values of the diagnostic criteria for the different diagnosis. Each data bar represents the mean value of the selected criterion for all spectra of the corresponding histopathology. The error bars represent the range of deviation (min to max) from the mean value. In graph (a) the data bars correlate the UV-visible ESS diagnostic criterion (area difference between the spectra and the trapezoid formed at the boundaries of the range of 400 to 650 nm) to the histopathological findings. In graph (b) the data bars correlate the NIR ESS diagnostic criterion (area under the curve for the range of 920 to 1200 nm in the normalized spectra) to the histopathological findings.

ing effects. We note that our data are at odds with the melanoma spectra reported by Wallace et al., which showed high melanin absorption in the UV-visible band.[43] This is likely a consequence of the use of a different probe geometry (a bundle of 30 source-detector fibers with a range of separations and cross talk effects), which would be less sensitive to scattering changes. Their benign-lesion spectra were relatively featureless except for the attenuation at shorter wavelengths, which is consistent with the known absorption by melanin, and with a smaller effect from scattering.

In a global analysis, Fig. 4(a) shows strong spectral trends, which result in clear groupings, and is suggestive of possible future diagnostic algorithms to be tested in humans. Based on the spectral shapes for the different lesions, we found that the range of 400 to 650 nm provided one of the most significant differences between benign lesions and melanomas. The area difference between the trapezoid formed at the boundaries of this range and the corresponding spectral curve was used to distinguish malignant melanomas from benign lesions for UV-visible ESS. The normal skin was not considered in the analysis because the clinically interesting problem is to distinguish between benign and malignant lesions.

The graph of Fig. 5(a) shows the mean values of this parameter for the different pathology classifications. The error bars represent the full range of deviation from the mean value. The UV-visible ESS provided good correlation for 11/13 lesions. Two ''misclassified'' lesions grouped spectrally with malignant melanomas. However, it is important to underline here that one of them was classified undecided by the histopathological assessment. The other one was classified benign.

As shown in the close view of Fig. 4(b), the NIR-ESS scatter spectra represent pigmented benign lesions, melanomas, and normal skin. The spectra were normalized to the total area under the entire curve. The spectra are the averages of each of the three types of examined tissues. The common feature among the three tissue types is the broad absorption band due to water at around 1450 nm. The full width at half maximum (FWHM) of the melanoma scatter spectrum in the range of 920 to 1400 nm is significantly larger than that of benign lesions. Moreover, a small feature around 1150 nm also distinguishes the melanoma spectra from those of benign nevi. For the analysis, the NIR-ESS spectra were renormalized to unity at the wavelength 1340 nm, chosen because there is minimal water absorption at this wavelength. The area under the curve covering the range of 920 to 1200 nm in the normalized spectra was chosen as the distinction criterion. Again, the normal skin was not included in this analysis. The spectrum for normal skin shows a small absorption feature due to water, around 1200 nm, which does not appear either in benign lesions or melanomas. This is consistent with deeper sampled depth in normal skin due to lower scattering without melanin.

In Fig. 5(b) the data bars represent the mean value of the 920 to 1200 area criterion for each corresponding diagnosis. The error bars represent the full range of deviation from the mean value for each corresponding histopathology. As in Fig. 5(a), the area criterion is correlated to the histopathological findings. Using the area (920 to 1200 nm) distinction criterion, NIR-ESS showed good correlation for 12/13 lesions. The ''misclassified'' lesion grouped with the benign lesions spectrally; however, it was classified undecided by the histopathological assignment.

Table 1 summarizes the findings of the standard histopathological procedure in comparison with the results obtained by both ESS systems. Analysis of these data shows that both UV-visible and NIR elastic scattering spectroscopy provide spectral criteria that correlate with the histopathological findings. The UV-visible ESS correctly classified 85% of the examined lesions, whereas the NIR-ESS correctly classified 92%. Both UV-visible and NIR methods are sensitive to cellular morphology. As previously stated, our initial intent in testing NIR-ESS was to be more sensitive to changes in scattering, in a spectral region where the absorption coefficient of melanin would be minimized. It is expected that spectra of thicker lesions would be more distinguishable in the NIR range than in the UV-visible range. However, we believe that the differences in lesion thickness (depth) have only a modest effect on the ESS spectral data for melanocytic lesions, because so much of the signal (for this optical geometry) comes

Table 1 Comparison between the histopathological findings and ESS results.

Animal	Lesion	Histopathology findings	UV-visible ESS findings	NIR-ESS findings
1	1	Benign	Benign	Benign
	2	Benign	Benign	Benign
	3	Benign	Benign	Benign
	4	Normal skin	Normal skin	Normal skin
2	5	Benign	Melanoma	Benign
	6	Benign	Benign	Benign
	7	Benign	Benign	Benign
3	8	Melanoma	Melanoma	Melanoma
	9	Melanoma	Melanoma	Melanoma
	10	Melanoma	Melanoma	Melanoma
4	11	Undecided	Melanoma	Benign
	12	Melanoma	Melanoma	Melanoma
	13	Melanoma	Melanoma	Melanoma

from scatterers at shallow depths (<400 μm). Both UV-visible and NIR ranges are sensitive to the melanosomes, which are the strongest subcellular scatterers in pigmented lesions.

Studies on human subjects, with a larger statistical set, have been initiated by our clinical collaborators at University College London Hospital to establish statistical validity of the ESS technique for diagnosis of pigmented skin lesions. Preliminary results using UV-visible ESS indicates spectral trends in human melanomas similar to those found in opossum melanomas.[53]

4 Conclusions

ESS is a sensitive technique for detecting changes in subcellar morphology that accompany the transformation of normal cells to cancerous cells. The results of the experiment on opossums show that both UV-visible and NIR-ESS have the potential to classify pigmented skin lesions with encouraging spectral trends that correlate with standard histopathological examination. NIR-ESS correctly classified one more lesion than did UV-ESS in correlation with histopathology, but both wavelength regions appear equally promising. Although encouraging, ultimate utility cannot yet be determined from such a small dataset, and larger studies are planned to statistically substantiate the efficacy of ESS for diagnosis of pigmented skin lesions in humans.

Acknowledgments

The authors would like to thank Dr. D. K. Kusewitt (Ohio State University, College of Medicine and Public Health) for the histopathology analysis.

References

1. R. M. MacKie, D. Hole, J. A. Hunter, R. Rankin, A. Evans, K. McLaren, M. Fallowfield, A. Hutcheon and A. Morris, ''Cutaneous malignant melanoma in Scotland: incidence, survival, and mortality, 1979–94. The Scottish Melanoma Group,'' *Br. Med. J.* **315**, 1117–1121 (1997).
2. G. G. Giles, B. K. Armstrong, R. C. Burton, M. P. Staples, and V. J. Thursfield, ''Has mortality from melanoma stopped rising in Australia? Analysis of trends between 1931 and 1994,'' *Br. Med. J.* **312**, 1121–1125 (1996).
3. J. F. Aitken, J. M. Elwood, J. B. Lowe, D. W. Firman, K. P. Balanda, and I. T. Ring, ''A randomised trial of population screening for melanoma,'' *J. Med. Screen.* **9**, 33–37 (2002).
4. S. L. Edwards and K. Blessing, ''Problematic pigmented lesions: approach to diagnosis,'' *J. Clin. Pathol.* **53**(6), 409–418 (2000).
5. S. C. Chen, D. M. Bravata, E. Weil, and I. Olkin, ''A comparison of dermatologists' and primary care physicians' accuracy in diagnosing melanoma,'' *Arch. Dermatol.* **137**, 1627–1634 (2001).
6. M. Elbaum, A. W. Kopf, H. S. Rabinovitz, R. G. B. Langley, H. Kamino, M. C. Mihm, A. J. Sober, G. L. Peck, A. Bogdan, D. Gutkowicz-Krusin, M. Greenebaum, S. Keem, M. Oliviero, and S. Wang, ''Automatic differentiation of melanoma from melanocytic nevi with multispectral digital dermoscopy: A feasibility study,'' *J. Am. Acad. Dermatol.* **44**(2), 207–218 (2001).
7. A. Bono, S. Tomatis, C. Bartoli, G. Tragni, G. Radaelli, A. Maurichi, and R. Marchesini, ''The ABCD system of melanoma detection: a spectrophotometric analysis of the asymmetry, border, colour, and dimension,'' *Cancer* **85**, 72–77 (1999).
8. A. Bono, S. Tomatis, C. Bartoli, N. Cascinelli, C. Clemente, C. Cupeta, and R. Marchesini, ''The invisible colours of melanoma. A Telespectrophotometric diagnostic approach on pigmented skin lesions,'' *Eur. J. Cancer* **32A**(4), 727–729 (1996).
9. S. Tomatis, C. Bartoli, A. Bono, N. Cascinelli, C. Clemente and R. Marchesini, ''Spectrophotometric imaging of cutaneous pigmented lesions: discriminant analysis, optical properties and histological characteristics,'' *Photochem. Photobiol.* **42**(1), 32–39 (1998).
10. B. Farina, C. Bartoli, A. Bono, A. Colombo, M. Lualdi, G. Trani and R. Marchesini, ''Multispectral imaging approach in the diagnosis of cutaneous melanoma: potentiality and limits,'' *Phys. Med. Biol.* **45**(5), 1243–1254 (2000).
11. S. W. Menzies, C. Ingvar, and W. H. McCarthy, ''A sensitivity and specificity analysis of the surface microscopy features of invasive melanoma,'' *Melanoma Res.* **6**, 55–62 (1996).
12. S. W. Menzies, A. Gustenev, M. Avramidis, A. Batrac, and W. H. McCarthy, ''Short-term digital surface microscopic monitoring of atypical or changing melanocytic lesions,'' *Arch. Dermatol.* **137**, 1583–1589 (2001).
13. P. Carli, V. De Giorgi, and B. Giannotti, ''Dermoscopy and early diagnosis of melanoma,'' *Arch. Dermatol.* **137**, 1641–1644 (2001).
14. P. Anikijenko, L. T. Vo, E. R. Murr, J. Carrasco, W. J. McLaren, Q. Chen, S. G. Thomas, P. M. Delaney, and R. G. King, ''In vivo detection of small subsurface melanomas in athymic mice using noninvasive fiber optic confocal imaging,'' *J. Invest. Dermatol.* **117**(6), 1442–1448 (2001).
15. S. Andersson-Engels and B. C. Wilson, ''In vivo fluorescence in clinical oncology: Fundamental and practical issues,'' *J. Cell Pharmacol.* **3**, 66–79 (1992).
16. I. J. Bigio and J. R. Mourant, ''Ultraviolet and visible spectroscopies for tissue diagnostics: fluorescence spectroscopy and elastic-scattering spectroscopy,'' *Phys. Med. Biol.* **42**, 803–813 (1997).
17. G. A. Wagnières, W. M. Star, and B. C. Wilson, ''In vivo fluorescence spectroscopy and imaging for oncological applications,'' *Photochem. Photobiol.* **68**(5), 603–632 (1998).
18. G. J. Tearney, M. E. Brezinski, B. E. Bouma, S. A. Boppart, C. Pitris, J. E. Southern, and J. G. Fujimoto, ''In vivo endoscopic optical biopsy with optical coherence tomography,'' *Science* **276**(3321), 2037–2039 (1997).
19. S. B. Colak, M. B. van der Mark, G. W. Hooft, J. H. Hoogenraad, E. S. van der Linden, and F. A. Kuijpers, ''Clinical optical tomography and NIR spectroscopy for breast cancer detection,'' *IEEE J. Sel. Top. Quantum Electron.* **5**(4), 1143–1158 (1999).
20. S. Jackle, N. Gladkova, F. Fledchtein, A. Terentieva, B. Brand, G. Gelikonov, V. Gelikonov, A. Sergeev, A. Fritscher-Ravens, J. Freund, U. Seitz, S. Schroder, and N. Soehendra, ''In vivo endoscopic optical coherence tomography of esophagitis, Barrett's esophagus, and ad-

enocarcinoma of the esophagus,'' *Endoscopy* **32**(10), 750–755 (2000).
21. H. Liu, D. Boas, Y. Zhang, A. G. Yodh, and B. Chance, ''Determination of optical properties and blood oxygenation in tissue using continuous NIR light,'' *Phys. Med. Biol.* **40**(11), 1983–1993 (1995).
22. M. J. Holboke, B. Tromberg, X. Li, N. Shah, J. Fishkin, D. Kidney, J. Butler, B. Chance, and A. G. Yodh, ''Three-dimensional diffuse optical mammography with ultrasound localization in a human subject,'' *J. Biomed. Opt.* **5**(2), 237–247 (2000).
23. A. E. Cerussi, D. Jakubowski, N. Shah, F. Bevilacqua, R. Lanning, A. J. Berger, D. Hsiang, J. Butler, R. F. Holocombe, and B. J. Tromberg, ''Spectroscopy enhances the information content of optical mammography,'' *J. Biomed. Opt.* **7**(1), 60–71 (2002).
24. G. C. Tang, A. Pradhan, and R. R. Alfano, ''Spectroscopic differences between human cancer and normal lung and breast tissues,'' *Lasers Surg. Med.* **9**, 290–295 (1989).
25. N. N. Boustany, R. Manoharan, R. R. Dasari, and M. S. Feld, ''Analysis of normal and diseased colon mucosa using ultraviolet resonance Raman spectroscopy,'' *Proc. SPIE* **2679**, 66–70 (1996).
26. M. Gniadecka, P. Philipsen, L. Hansen, J. Hercogova, K. Rossen, H. Thomsen, and H. Wulf, ''Malignant melanoma diagnosis by Raman spectroscopy and artificial neural network,'' *J. Invest. Dermatol.* **113**(3), 464 (1999).
27. G. Zonios, L. T. Perelman, V. Backman, R. Manoharan, A. Nusrat, S. Shields, M. Fitzmaurice, J. Can Dam, and M. S. Feld, ''Diffuse reflectance spectroscopy of human adenomatous colon polyps in vivo,'' *Appl. Opt.* **38**, 6628–6637 (1999).
28. M. Osawa and S. Niwa, ''A portable diffuse reflectance spectrophotometer for rapid and automatic measurement of tissue,'' *Meas. Sci. Technol.* **4**, 668–676 (1993).
29. L. T. Perelman, V. Backman, M. Wallace, G. Zonios, R. Manoharan, A. Nusrat, S. Shields, M. Seiler, C. Lima, T. Hamano, I. Itzkan, J. Can Dam, J. M. Crawford, and M. S. Feld, ''Observation of periodic fine structure in reflectance from biological tissue: a new technique for measuring nuclear size distribution,'' *Phys. Rev. Lett.* **80**, 627–630 (1998).
30. J. C. E. Underwood, ''General and systemic pathology,'' Chap. 24 in *Skin*, pp. 667–697, Churchill Livingstone (2000).
31. I. J. Bigio, S. G. Bown, G. M. Briggs, M. Gavin, C. Kelley, S. Lakhani, D. Pickard, P. M. Ripley, I. Rose, and C. Saunders, ''Diagnosis of breast cancer using elastic-scattering spectroscopy: preliminary clinical results,'' *J. Biomed. Opt.* **5**, 221–228 (2000).
32. J. R. Mourant, I. J. Bigio, J. Boyer, T. M. Johnson, J. A. Lacey, A. G. Bohorfoush, and M. Mellow, ''Elastic-scattering spectroscopy as a diagnostic tool for differentiating pathologies in the gastrointestinal tract: preliminary testing,'' *J. Biomed. Opt.* **1**(2), 192–199 (1996).
33. D. C. Pickard, L. B. Lovat, M. Novelli, P. M. Ripley, C. Kelly, I. J. Bigio, and S. G. Bown, ''Diagnosis of dysplasia in Barrett's oesophagus with in-situ elastic-scattering spectroscopy,'' *Proc. SPIE* **4161**, 122–130 (2000).
34. J. R. Mourant, I. J. Bigio, J. Boyer, R. L. Conn, T. M. Johnson, and T. Shimada, ''Spectroscopic diagnosis of bladder cancer with elastic light scattering,'' *Lasers Surg. Med.* **17**, 350–357 (1995).
35. J. D. Whited and J. M. Grichnik, ''Clinical diagnosis of moles vs melanoma,'' *J. Am. Med. Assoc.* **280**(10), 881–882 (1998).
36. R. R. Mehta, L. Bratescu, J. M. Graves, A. Shilkaitis, A. Green, R. G. Mehta, and T. K. Das Gupta, ''In vitro transformation of human congenital naevus to malignant melanoma,'' *Melanoma Res.* **12**(1), 27–33 (2002).
37. A. Jackson, C. Wilkinson, M. Ranger, R. Pill, and P. August, ''Can primary prevention or selective screening for melanoma be more precisely targeted through general practice? A prospective study to validate a self administered risk score,'' *Br. Med. J.* **316**, 7124–7134 (1998).
38. J. F. Aitken, J. M. Elwood, J. B. Lowe, D. W. Firman, K. P. Balanda, and I. T. Ring, ''A randomised trial of population screening for melanoma,'' *J. Med. Screen* **9**, 33–37 (2002).
39. C. M. Balch, S. J. Soong, J. E. Gershenwald, J. F. Thompson, D. S. Reintgen, N. Cascinelli, M. Urist, K. M. McMasters, M. I. Ross, J. M. Kirkwood, M. B. Atkins, J. A. Thompson, D. G. Coit, D. Byrd, R. Desmond, Y. Zhang, P. Y. Liu, G. H. Lyman, and A. Morabito, ''Prognostic factors analysis of 17,600 melanoma patients: validation of the American Joint Committee on Cancer Melanoma Staging System,'' *J. Clin. Oncol.* **19**(16), 3622–3634 (2001).
40. R. Marchesini, C. Clemente, E. Pignoli, and M. Brambilla, ''Optical properties of in vitro epidermis and their possible relationship with optical properties of in vivo skin,'' *Photochem. Photobiol.* **16**(2), 127–140 (1992).
41. G. Zonios, J. Bykowski, and N. Kollias, ''Skin melanin, hemoglobin and light scattering properties can be quantitatively assessed in vivo using diffuse reflectance spectroscopy,'' *J. Invest. Dermatol.* **117**(6), 1452–1457 (2001).
42. M. L. Wolbarsht, A. W. Walsh, and G. George, ''Melanin, a unique biological absorber,'' *Appl. Opt.* **20**, 2184–2186 (1981).
43. V. P. Wallace, D. C. Crawford, P. S. Mortimer, R. J. Ott and J. C. Bamber, ''Spectrophotometric assessment of pigmented skin lesions: methods and feature selection for evaluation of diagnostic performance,'' *Phys. Med. Biol.* **45**(3), 735–751 (2000).
44. V. P. Wallace, J. C. Bamber, D. C. Crawford, R. J. Ott, and P. S. Mortimer, ''Classification of reflectance spectra from pigmented skin lesions, a comparison of multivariate discriminant analysis and artificial neural networks,'' *Phys. Med. Biol.* **45**(10), 2859–2871 (2000).
45. L. M. McIntosh, R. Summers, M. Jackson, H. H. Mantsch, J. R. Mansfield, M. Howlett, A. N. Crowson, and J. W. P. Toole, ''Towards non-invasive screening of skin lesions by near-infrared spectroscopy,'' *J. Invest. Dermatol.* **116**, 175–181 (2001).
46. D. E. Kusewitt, L. A. Applegate, and R. D. Ley, ''Ultraviolet radiation-indueced skin tumors in a South American opossum (Monodelphis domestica),'' *Vet. Pathol.* **28**(1), 55 (1991).
47. J. R. Mourant, T. Fuseilier, J. Boyer, T. M. Johnson, and I. J. Bigio, ''Predictions and measurements of scattering and absorption over broad wavelength ranges in tissue phantoms,'' *Appl. Opt.* **36**(4), 949–957 (1997).
48. J. R. Mourant, I. J. Bigio, D. A. Jack, T. M. Johnson, and H. D. Miller, ''Measuring absorption coefficients in small volumes of highly scattering media: source-detector separation for which path lengths do not depend on scattering properties,'' *Appl. Opt.* **36**(22), 5655–5661 (1997).
49. T. Sarna and H. M. Swartz, ''The physical properties of melanins,'' in *The Pigmentary System*, J. J. Nordlund, R. E. Boissy, V. J. Hearing, R. A. King and J.-P. Orotonne, Eds., Oxford University Press, UK (1988).
50. D. F. Kusewitt, L. A. Applegate, C. D. Bucana, and R. D. Ley, ''Naturally occurring malignant melanoma in the South American opossum (Monodelphis domestica),'' *Vet. Pathol.* **27**, 66–68 (1990).
51. H. Y. Thong, S. H. Jee, C. C. Sun, and R. E. Biossy, ''The paterns of melanosomes distribution in keratinocytes of human skin as one determining factor of skin color,'' *British J. Dermatol.* **149**, 498–505 (2003).
52. N. Nagai, Y. J. Lee, N. Nagaoka, M. Gunduz, K. Nojima, H. Tsujigiwa, E. Gunduz, C. H. Siar, and H. Nagatsuka, ''Elemental sulphur and alkali elutable melanin detected in oral melanosis and malignant melanoma by energy-filtering transmission electron microscopy,'' *J. Oral Pathol. Med.* **31**, 481–487 (2002).
53. J. J. Scarisbrick, C. D. O. Pickard, A. C. Lee, G. M. Briggs, K. Johnson, S. G. Bown, M. Novelli, M. R. S. Keshtgar, I. J. Bigio, and R. Yu, ''Elastic scattering spectroscopy in the diagnosis of pigmented lesions: Comparison with clinical and histopathological diagnosis,'' *Proc. SPIE* **5141**, 147–156 (2003).